Electronic properties of the ordered metallic Mn:Ge(111) interface

L. Sangaletti,[1] D. Ghidoni,[1] S. Pagliara,[1] A. Goldoni,[2] A. Morgante,[3,4] L. Floreano,[3] A. Cossaro,[3] M. C. Mozzati,[5] and C. B. Azzoni[5]

[1]*INFM and Universitá Cattolica, via dei Musei 41, 25121 Brescia, Italy*

[2]*Sincrotrone Trieste S.C.P.A., Basovizza, Trieste, Italy*

[3]*Laboratorio TASC-INFM, Basovizza, Trieste, Italy*

[4]*Dipartimento di Fisica, Universitá di Trieste, via Valerio 2, 34127 Trieste, Italy*

[5]*CNISM and Dipartimento di Fisica "A. Volta", Universitá di Pavia, via Bassi 6, 27100 Pavia, Italy*

(Received 26 November 2004; revised manuscript received 28 February 2005; published 12 July 2005)

The electronic and structural properties of an Mn:Ge(111) ordered interface produced by annealing Mn multilayers evaporated on a Ge(111) single crystal have been investigated. After annealing above 300 K, the surface always showed a $(\sqrt{3}\times\sqrt{3})$R30° reconstruction. The interface obtained after the evaporation of 4 ML has been selected for electronic spectroscopy studies, while thicker layers have been prepared for magnetization measurements. A ferromagnetic ordering with a T_c of about 260 K was detected. The Mn $2p$ XAS and XPS spectra indicate that the Mn:Ge(111) interface is metallic, and resonant photoemission spectra collected across the Mn $2p\rightarrow 3d$ absorption edge display characteristic many-electron effects for the Mn spectral weight in the valence band, with a significant contribution of Mn-derived states at the Fermi edge.

DOI: 10.1103/PhysRevB.72.035434 PACS number(s): 79.60.Dp, 78.70.Dm, 68.47.Fg, 61.14.Hg

I. INTRODUCTION

Recent investigations on the Mn—Ge systems have evidenced a ferromagnetic ordering in both single crystals,[1,2] and thin film alloys[3] which make them suitable for applications in the field of spintronics. Indeed, Ge presents intrinsic hole mobilities higher than either GaAs or Si, being a large hole concentration essential to mediate the ferromagnetic exchange which determines the magnetic properties of the sample.[4] Due to the remarkable magnetic properties, there is also a growing interest in the study of the structural properties of both Mn/Ge(100) and Mn/Ge(111) interfaces,[5–8] which are fundamental for the epitaxial growth of ferromagnetic layers on Ge single crystals. The study of these ultrathin layers is also related with the recently reported preparation of 50 nm thick Mn_5Ge_3 layers epitaxially grown onto the Ge(111) surface.[9] It was shown that the $(\sqrt{3}\times\sqrt{3})$R30° surface reconstruction of the Mn:Ge(111) interface can be considered as the seed structure for growing ferromagnetic Mn_5Ge_3 epitaxial layers. According to Zeng *et al.*,[9,10] the appearance of a $(\sqrt{3}\times\sqrt{3})$R30° symmetry in the surface structure can be unequivocally associated with the formation of an Mn_5Ge_3 ordered phase, exposing the Mn-terminated (0001) surface. Due to the reduced lattice mismatch (3.7%) between the hexagonal Mn_5Ge_3 (001) surface and the $(\sqrt{3}\times\sqrt{3})$R30° Ge(111) reconstructed surface, the Mn_5Ge_3 ordered phase can develop from the seed layer obtained at the early stages of Mn evaporation into a bulklike phase with thickness up to tens of nm.

The interest in the epitaxial growth of Mn/semiconductor interfaces has also important implications for the case of Mn silicides. Indeed, a recent study on thin manganese films on Si(111)-(7×7) reports on the formation of a metallic phase provided that the surface shows a $(\sqrt{3}\times\sqrt{3})$R30° reconstruction, while the (1×1) reconstructed surface displays a semiconducting character.[11]

While most studies on the Mn:Ge systems have been devoted to the preparation of epitaxial layers or single crystals and to the measurement of their magnetic and transport properties, the studies on the electronic properties are still mainly on a theoretical stage.[12–16] An investigation of the electronic properties of the system is fundamental to address some open questions, such as electron correlation effects, metallic or semiconducting properties, and the origin of the charge carriers. In this respect, photoemission spectroscopies are playing a central role in the study of diluted magnetic semiconductors (DMS) since in resonance conditions they can provide information on the contribution of magnetic ions to the spectral weight in the valence band region. Indeed, several experiments have been recently reported on resonant photoemission (RESPES) at the Mn $np\rightarrow 3d$ ($n=2,3$) absorption edge of DMS compounds.[17–20] These studies contributed to elucidate the origin of the electronic states in the valence band region and, in particular, the distribution of the Mn $3d$ spectral weight.

From the analysis of recent experimental and theoretical works, two endpoints can be identified in the growth of Mn on Ge(111). In the low-coverage limit (i.e., less than 1 ML) a surface structure related to the $c(2\times8)$ reconstruction of the Ge(111) surface,[8] as well as a 1/3 ML of Mn on the Ge(111) $(\sqrt{3}\times\sqrt{3})$R30° reconstructed surface,[13] have been considered, while in the limit of high coverages (i.e., 50 nm) the Mn_5Ge_3 epitaxial phase has been produced.[9]

Our study explores an intermediate regime (4 to 190 ML), where the Mn:Ge(111) surface is always found to be metallic and displays a structural ordering identified by the $(\sqrt{3}\times\sqrt{3})$R30° surface reconstruction. The electronic structure of the Mn/Ge(111) interface is probed by high energy photoemission and x-ray absorption spectroscopies. The analysis of resonant photoemission spectra collected across the Mn $2p\rightarrow 3d$ absorption threshold allowed us to single out the spectral weight of the Mn states in the valence band region

with a significant emission at the Fermi edge. In the thicker layer the sample shows ferromagnetic properties with a transition at $T_c = 260$ K.

II. EXPERIMENT

For this experiment the (111) surface of Ge single crystals has been used as substrate for the deposition of the Mn atoms. The crystal surface was prepared by repeated cycles of Ar ion sputtering at 1 keV beam energy and annealing at 700 °C until a sharp RHEED pattern was obtained, displaying the characteristic $c(2\times 8)$ symmetry reconstruction of the clean surface.

Mn layers were deposited at room temperature by in-situ electron beam evaporation from a Mo crucible with a constant flux of Mn ions. The surface electronic structure has been studied for several samples obtained after an evaporation of 4 up to 190 ML thick Mn film on the (111) surface of a Ge single crystal. Post-growth annealing was carried out from 300 °C to 500 °C for 120 seconds to induce the surface alloy formation. The thickness of the overlayers was measured by x-ray reflectivity and by considering the attenuation length of photoemitted electrons. All these probes gave thickness values consistent with those obtained from a calibrated thickness monitor.

In the present study we will focus on the sample obtained after an Mn evaporation of 4 ML. Annealing of this sample produced a Mn:Ge(111) reacted interface with a thickness of about 7 Å, as estimated by considering the attenuation of the Mn $2p$ photoemission intensity after the annealing. Thicker layers with the same structural properties detected in the 4 ML sample were produced for *ex-situ* magnetic measurements.

In photoemission experiments, the RESPES spectra were collected by scanning the photon energy from $h\nu = 636$ to 657 eV through the Mn $2p$-$3d$ absorption threshold. Additional photoemission spectra were collected with a photon energy of 840 eV, in order to control surface contaminations and estimate the thickness of the annealed layers. The measurements have been performed at the INFM ALOISA synchrotron beamline in Trieste (Italy). The experimental setup is described in details elsewhere.[19,21] Static magnetization of the sample was measured at 1000 Oe from 352 K to 2 K with a SQUID Quantum Design magnetometer. Magnetization loops at different temperatures were also collected for fields ranging between 0 and 5000 Oe. Magnetization measurements were carried out on the ordered film obtained after an Mn evaporation of 50 ML and subsequent annealing.

III. RESULTS AND DISCUSSION

A. Surface structural properties

The process leading to the formation of a surface phase was monitored by observing the evolution of RHEED patterns during annealing. The $c(2\times 8)$ RHEED pattern of the reconstructed Ge(111) surface disappeared just after the Mn evaporation and before annealing. As temperature increased during the annealing, the coexistence of different phases was observed [i.e., $(\sqrt{3}\times\sqrt{3})$R30°, $c(2\times 8)$], while after annealing just above 300 °C, only the $(\sqrt{3}\times\sqrt{3})$R30° reconstructed surface was observed, which is a proof the surface homogeneity. More important for the present investigation is the fact that only annealed surfaces show a structural order. This indicates that Mn does interact with the Ge substrate to yield a reconstructed surface and strongly suggests that the Mn spectral weight detected from the ordered interface by electron spectroscopy probes is not coming from unreacted metallic Mn.

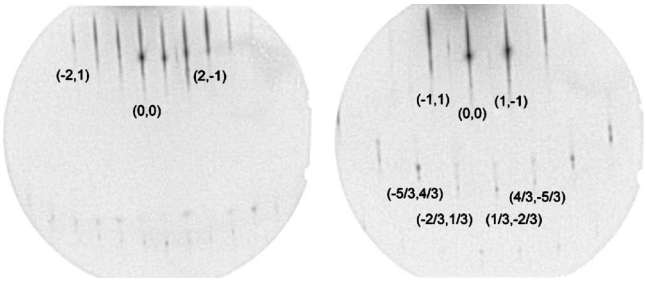

FIG. 1. Left, RHEED pattern of the Mn:Ge(111) surface phase obtained after a Mn evaporation of 4 ML, taken with the electron beam along the ⟨112⟩ substrate direction. The specularly reflected spot (0,0) and the first integer spots $(-2,1)$ and $(2,-1)$ are individually labeled. Fractional order spots appear in between the specular and first integer spots, due to the Mn induced $(\sqrt{3}\times\sqrt{3})$R30° surface reconstruction. Right, RHEED pattern of the Mn:Ge(111) surface phase taken with the electron beam along the ⟨110⟩ substrate direction. Third-integer order spots are also labeled.

The $(\sqrt{3}\times\sqrt{3})$R30° patterns obtained after annealing above 300 °C have been detected for different Mn coverages, from 4 to 190 ML. In the present study the spectroscopic results from surfaces displaying only the $(\sqrt{3}\times\sqrt{3})$R30° reconstructions have been selected.

The RHEED patterns of the Mn:Ge(111) interface obtained after a Mn evaporation of 4 ML are shown in Fig. 1 along the ⟨112⟩ and ⟨110⟩ directions (left and right panel, respectively). The reconstruction displays a $(\sqrt{3}\times\sqrt{3})$R30° symmetry, whose fractional spots can be seen along the ⟨112⟩ direction (cf. RHEED images in Ref. 22). This symmetry reconstruction is rather common upon absorption of isovalent elements[23,24] and several other metals.[23,25] From the width of the RHEED fractional spots we can estimate an average domain size of several nanometers (6–7 nm). This might be equally due to the presence of Mn-vacancy defects which release the strain over the surface, as evidenced by Zeng *et al.*,[10] or to a relative increase of the surface roughness. However, we can exclude the presence of residual Mn clusters above the surface of the Mn:Ge(111) system, since we never detected any evidence of the characteristic spots of a transmission electron diffraction pattern due to 3D clusters or large roughness. Finally, by comparison with previous structural studies,[9,10] we can associate the $(\sqrt{3}\times\sqrt{3})$R30° surface symmetry that we have observed for thicker layers, with the formation of a bulk Mn_5Ge_3 ordered phase exposing the (0001) surface.

B. Magnetic properties

In Fig. 2 the "in-plane" magnetic moment of the Mn:Ge(111) interface as a function of temperature is shown,

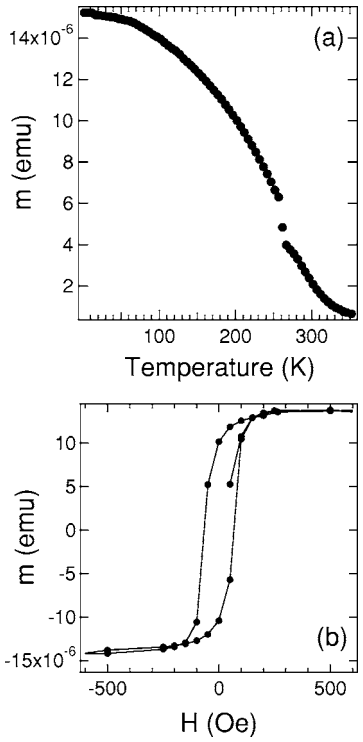

FIG. 2. (a) Magnetic moment vs T curve of the 190 ML thick film. (b) Hysteresis loop measured in plane at $T=50$ K.

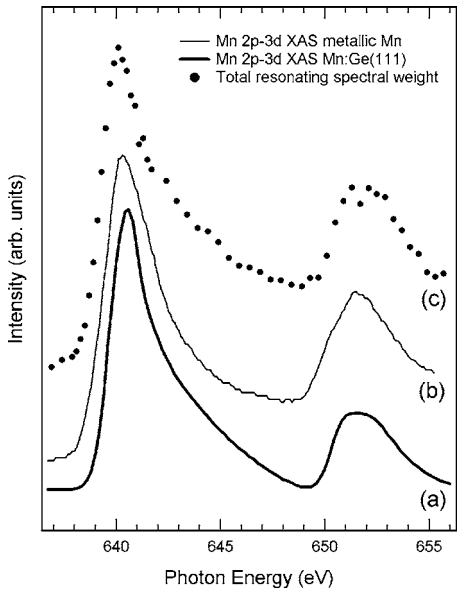

FIG. 3. Mn L-edge XAS spectra of the Mn:Ge(111) alloy obtained after the evaporation of 4 ML thick Mn film (a), metallic Mn (b) (Ref. 27), and total resonating spectral weight extracted from the RESPES data of Fig. 4(c).

along with the hysteresis cycle measured at 50 K with the external magnetic field applied parallel to the layer surface. The m vs T curve, measured under an applied field of 1000 Oe, shows a paramagnetic to ferromagnetic transition at about 260 K. The antiferromagnetism of the α-Mn phase at 95 K (Ref. 26) is not observed, indicating that on a "bulk" sensitive scale the system does not show the presence of a detectable metallic Mn phase. Also the contribution of $Mn_{11}Ge_8$, which is antiferromagnetic below 145 K (Ref. 9) is ruled out by our magnetization measurements.

C. X-ray absorption spectroscopy

In Fig. 3(a) the XAS spectrum of the 4 ML-thick Mn:Ge(111) interface is shown. The spectrum is compared to that collected from metallic Mn [Fig. 3(b)].[27] As can be observed, the Mn XAS profile shows spectral features close to those measured on metallic Mn, with two broad spin-orbit split lines.

In Fig. 3(c) the total resonating spectral weight is also shown (dots). This profile has been extracted by plotting, for each photon energy, the sum of the normal Auger emission and the resonant Mn $3d$ spectral weight. In this respect, it can be considered as a partial yield spectrum collected in a kinetic energy window ranging from 0 to 20 eV below the photon energy. Also this spectrum has a line shape comparable to the XAS of metallic Mn.

In metals, one-electron band widths and/or hybridization effects can mix the possible local electronic configurations yielding a breakdown of an atomic description of the electronic structure. This may happen because of fluctuations of d-electron count or mixing of various possible states of d^n atomic configurations. These effects are evident in the trend observed for the Mn $2p$-$3d$ XAS spectrum of metallic Mn (Ref. 27), and the Mn $2p$ EELS spectrum of Mn as impurity in Cu or Ag reported by Thole *et al.*[28] Indeed, while Mn in Ag shows well resolved components of the Mn $2p_{3/2}$ and Mn $2p_{1/2}$ regions, the relatively stronger hybridization with the Cu sp conduction band and the mixing with the d^6 configuration makes the spectral features broader, although the fine structure arising from the Mn^{2+} configuration is still detectable. Finally, as is the case of the present compound, the XAS fine structure of metallic Mn is completely quenched by the simultaneous contribution of several configurations and fluctuating $3d$ electron count.

Also the line shape of the Mn $2p$ XPS spectrum (not shown here) is similar to that of metallic Mn, with no evidence of either the atomiclike fine structure of multiplet-split states of, e.g., MnO (Ref. 29) or the charge-transfer related satellites detected in DMS compounds.[30] However, it is important to observe that the Mn $2p$ line shape of different metallic (and mostly ferromagnetic) compounds containing a Mn ion sublattice can present different fine structures and widths,[31,32] including a Mn-metal-like spectrum similar to that we observe. For instance, in the case of Heusler alloys the line shape of Co_2MnSb displays a clear fine structure, while that of $La_{0.2}Sm_{0.8}MnSi_2$ is very similar to the line shape of metallic Mn.[32] Therefore, although in our case both the Mn $2p$ XAS and XPS line shapes are quite close to that of metallic Mn, several probes with different sensing depth (RHEED, SQUID magnetometry) show that Mn is forming an ordered Mn:Ge(111) interface and produces ferromagnetism in the layers, excluding the presence of metallic Mn within the spectroscopic sensitivity.

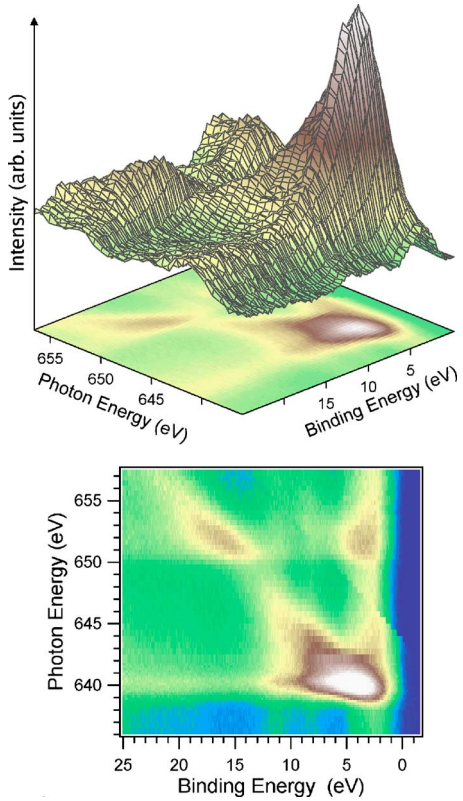

FIG. 4. (Color online) Resonant photoemission (RESPES) spectra of the Mn:Ge(111) interface collected at the Mn $2p$-$3d$ absorption edge. The interface was obtained after a Mn evaporation of 4 ML. In both panels the intensity of each photoemission spectrum is plotted in a 0 to 25 eV binding energy range, while the sequence of photoemission spectra have been collected by sweeping the photon energy from below the Mn L_{III} absorption threshold ($h\nu$=636 eV) to above the Mn L_{II} threshold at $h\nu$=657 eV.

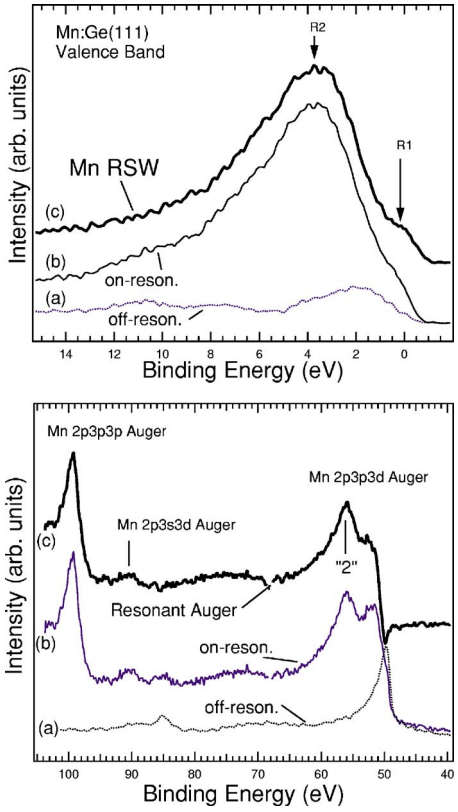

FIG. 5. (Top) Mn RSW [thick line (c)] obtained by subtracting the spectrum collected off-resonance [dotted line (a)] from the spectrum collected at resonance [thin line (b)]; (bottom) Mn $2p3p3p$, $2p3s3d$, and $2p3p3d$ resonant Auger emission [thick line (c)] obtained by subtracting from the spectrum collected at resonance [thin line (b)] the spectrum collected off-resonance [dotted line (a)].

D. Resonant photoemission spectroscopy

RESPES techniques are important tools to single out the contribution of open shell transition metal ions in strongly correlated systems. This is due to the strong enhancement of the $3d$ electrons spectral weight when photoemission experiments are carried out with photons that can excite an np electron to an unoccupied $3d$ level, leading to a process where two emission channels can be simultaneously present and can interfere with each other.[33] In particular, when RESPES experiments are carried out across the $2p \rightarrow 3d$ absorption threshold in $3d$ transition metal compounds, a dramatic enhancement of the electron emission is observed (see, e.g., Refs. 19, 20, 34, and 35 for the Mn case).

In Fig. 4 the RESPES data at the Mn L-threshold of our Mn:Ge(111) interface are shown. In the case of Mn $3d$ electrons, an interference between the direct photoemission channel, $2p^6\,3d^5+h\nu \rightarrow 2p^6\,3d^4+e_k$ and the Mn np-$3d$ excitation followed by a Coster-Kronig decay, $2p^63d^5+h\nu \rightarrow 2p^53d^6 \rightarrow 2p^63d^4+e_k$ occurs. As can be observed, the photoemission spectra collected across the Mn L_3 and L_2 thresholds show a considerable resonant behavior. At both resonance energies an intense emission is detectable at a binding energy (BE) of 4 eV. This emission shows a dispersive behavior on the BE scale (Fig. 4, bottom panel). This is the behavior expected for a normal Auger emission, which occurs when the electron excited into the empty states upon photon absorption promptly delocalizes and the system switches from a Raman-Auger emission to the normal-Auger emission (see, e.g., Ref. 36).

The possibility to distinguish Mn $3d$ derived states by RESPES at the Mn $2p \rightarrow 3d$ edge is particularly important for the region near the Fermi energy. Therefore, by subtracting from the resonant spectra collected with a $h\nu$ =640.5 eV photon the nonresonant spectrum collected with $h\nu$=636 eV, we have extracted the Mn contribution to the density of states in the valence band, hereafter denoted as Mn resonating spectral weight (RSW). The results are shown in Fig. 5, top panel. First, the Mn emission at the Fermi edge (R1 feature) should be observed, which makes the system a metallic surface alloy, in agreement with recent calculations[12–14,16] that predict a metallic behavior for the FM Mn_xGe_{1-x} bulk crystal or the Mn/Ge(111) interface. At odds with the theoretical predictions, the Mn spectral weight extends well below the Fermi edge, down to a BE of about 11 eV, which indicates that strong many-electron effects are present and affect the final state of the photoemission process. Indeed, no single-particle states of Mn are predicted at energies lower than 2–2.5 eV in Refs. 12–14 and 16. Moreover, the maximum intensity of the Mn RSW is detected at

about 4 eV (R2 feature), along with a shoulder on the high BE side, from 6 to about 11 eV. The simultaneous presence of a Fermi edge and of the Mn 3*d* localized states at 4 eV was also detected by Ishida *et al.*[37] in their study of the Mn-doped $ZnGeP_2$ single crystals. In this case, the Mn RSW was obtained by subtracting the normalized off-resonance (48 eV) spectrum from the on-resonance (51 eV) spectrum, collected across the Mn 3*p*-3*d* absorption threshold.

The electronic properties so far detected in the Mn:Ge(111) system are rather peculiar, and for the discussion of the origin of the observed spectral features a comparison with other alloys is required. In the past, a great effort has been devoted to study the electronic properties of Mn impurities in noble metals. More recently, surface alloys prepared by evaporating Mn atoms onto, e.g., Cu single crystals have been reported.[38,39] In these studies, the valence band of the $c2\times2$ CuMn/Cu(100) ordered surface alloy has been investigated with resonant photoemission. A peak at about 4 eV was singled out, which was ascribed to the majority Mn 3*d* emission. This feature can be related to the R2 emission in the Mn RSW we have singled out. Moreover, in Ref. 38 satellite structures were detected at 8 eV and 9.6 eV and ascribed to Mn states. In the present data, no clear evidence of this structure is found, unless one considers the shoulder ranging from about 6 to 11 eV in the Mn 3*d* RSW. However, our features, although located in a BE's range similar to those found for the $c2\times2$ CuMn/Cu(100) surface alloy, are larger, which could be ascribed to a higher degree of delocalization of the Mn 3*d* electronic states.

It is also rather interesting to make an analysis of the Mn $2p3p3p$ Auger emission at higher energies (about 97 eV) (Fig. 5, bottom panel). In this case, the resonant photoemission process leads to a final state with two Mn 3*p* holes with a multiplet structure characterized mainly by a singlet state at high energies (not shown in the present data) and a triplet state at low energies (97 eV), separated by about 10 eV. According to the analysis of Dürr *et al.*,[40] carried out on Mn ultrathin films on Cu(110) surfaces, the line shape of the triplet peak we have measured (Fig. 5, bottom panel) can be interpreted as that of an itinerant system. In fact, clustering and localization effects should give a twofold structure (due to the presence of both the unscreened $3p^43d^6$ and the screened $3p^43d^7$ configurations) with two peaks with comparable intensity, as observed for low coverage of Mn on metallic surfaces.[40] Therefore, we can assume that in our system the metallic character provides a pathway for electron delocalization which yields a single-peaked Mn $2p3p3p$ Auger emission.

Also the line shape of the Mn $2p3p3d$ Auger can be affected by localization effects as was shown for the Mn:Cu(110) interface.[41] In our case, the $2p3p3d$ Auger emission (Fig. 5, bottom panel) shows a dominant feature (which has been labeled as "2," as in Ref. 41). In the Mn:Cu(110) interface, peak "2" was ascribed to the better-screened $3p^53d^6$ final-state configuration, displaying a growth with increasing coverage. It was of equal intensity as the peak detected at higher BE's already at 0.5 ML coverage and became dominant at higher Mn coverages. The higher BE emission, which should be present at about 3 eV below peak 2, was ascribed to the unscreened $3p^53d^5$ final-state configuration and it was considered as a fingerprint of localization. In our case this emission is missing and, consistently with the findings on the Mn $2p3p3p$ line shape (see above), we conclude that our interface shows a prevalent metallic character.

Therefore, we may rule out localization effects at least for coverages larger than 4 ML. Further analysis about metallic (delocalized) character in the present system, could be developed in terms of Mn—Mn hybridization effects, which are ultimately dependent on the Mn—Mn distance, as proposed for MnSb.[42] Similar effects, which deserve further experimental and theoretical investigations, could also be expected for the Mn:Ge(111) interface.

IV. CONCLUSIONS

In conclusion, we have shown that ordered metallic Mn:Ge(111) surface alloys can be obtained by annealing a Ge (111) surface after the evaporation of 4 to 190 ML of metallic Mn. The surface layer is ordered with a $(\sqrt{3}\times\sqrt{3})$R30° reconstruction, which persists up to 190 ML, provided that the annealing temperature is kept between 300 °C and 500 °C. The Mn:Ge(111) interface shows a strong tendency to form a surface structure closely related to the Mn_5Ge_3 bulk crystals as that recently investigated by STM techniques,[10] rather than a diluted alloy as that prepared by Park *et al.*[3] and, more recently by Picozzi *et al.*[43] We started from a Mn thickness of 4 ML and we were able to grow ordered films up to 190 ML by several evaporation steps on the same crystal. These films were thick enough to allow SQUID magnetometry measurements, which resulted in a clear ferromagnetic phase below a T_c of about 260 K. The electronic properties of the layers have been studied by x-ray absorption and resonant photoemission spectroscopies. The Mn partial density of states, extracted from the resonant photoemission data as Mn RSW, displays a clear Fermi edge, but the spectral weight extends well below (about 11 eV) the Fermi edge, due to many-electron effects in the final state of the photoemission process. The energy position of the Mn 3*d* majority-spin emission is about 2 eV higher than that predicted by theoretical calculations. Finally there is not evidence of electron localization for layers obtained after a Mn evaporation larger than 4 ML. Our study poses a lower coverage limit for $(\sqrt{3}\times\sqrt{3})$R30° phases with delocalized electrons in the Mn:Ge(111) system and opens further studies of the electronic properties in the submonolayer regime which is virtually unexplored from an experimental point of view.

ACKNOWLEDGMENTS

L.S. and D.G. wish to acknowledge the financial support from the INFM-LdS project during the experiments at ELETTRA.

[1] Sunglae Cho, Sungyoul Choi, Soon Cheol Hong, Yunki Kim, J. B. Ketterson, Bong-Jun Kim, Y. C. Kim, and Jung-Hyun Jung, Phys. Rev. B **66**, 033303 (2002).
[2] H. Takizawa, T. Yamashita, K. Uheda, and T. Endo, J. Phys.: Condens. Matter **14**, 11147 (2002).
[3] Y. D. Park, A. T. Hanbicki, S. C. Erwin, C. S. Hellberg, J. M. Sullivan, J. E. Mattson, T. F. Ambrose, A. Wilson, G. Spanos, and B. T. Jonker, Science **295**, 651 (2002).
[4] See, e.g., H. Ohno, Science **281**, 951 (1998).
[5] N. Pinto, L. Morresi, R. Gunnella, R. Murri, F. D'Orazio, F. Lucari, S. Santucci, P. Picozzi, M. Passacantando, and A. Verna, J. Mater. Sci.: Mater. Electron. **14**, 337 (2003).
[6] N. Pinto, L. Morresi, R. Murri, F. D'Orazio, F. Lucari, M. Passacantando, and P. Picozzi, Phys. Status Solidi C **7**, 1748 (2004).
[7] R. Gunnella, L. Morresi, N. Pinto, R. Murri, L. Ottaviano, M. Passacantando, F. D'Orazio, and F. Lucari, Surf. Sci. **577**, 22 (2005).
[8] W. Zhu, H. H. Weitering, E. G. Wang, E. Kaxiras, and Z. Zhang, Phys. Rev. Lett. **93**, 126102 (2004).
[9] C. Zeng, S. C. Erwin, L. C. Feldman, A. P. Li, R. Jin, Y. Song, J. R. Thompson, and H. H. Weitering, Appl. Phys. Lett. **83**, 5002 (2003).
[10] C. Zeng, W. Zhu, S. C. Erwin, Z. Zhang, and H. H. Weitering, Phys. Rev. B **70**, 205340 (2004).
[11] A. Kumar, M. Tallarida, M. Hansmann, U. Starke, and K. Horn, J. Phys. D **37**, 1083 (2004).
[12] A. Stroppa, S. Picozzi, A. Continenza, and A. J. Freeman, Phys. Rev. B **68**,155203 (2003).
[13] G. Profeta, S. Picozzi, A. Continenza, and C. Franchini, Phys. Rev. B **70**, 155307 (2004).
[14] A. Continenza, F. Antoniella, and S. Picozzi, Phys. Rev. B **70**, 035310 (2004).
[15] S. Picozzi, A. Continenza, and A. J. Freeman, Phys. Rev. B **70**, 235205 (2004).
[16] J. Kudrnovsky, I. Turek, V. Drchal, F. Maca, P. Weinberger, and P. Bruno, Phys. Rev. B **69**, 115208 (2004).
[17] J. Okabayashi, T. Mizokawa, D. D. Sarma, A. Fujimori, T. Slupinski, A. Oiwa, and H. Munekata, Phys. Rev. B **65**, 161203(R) (2002).
[18] T. Mizokawa, T. Nambu, A. Fujimori, T. Fukumura, and M. Kawasaki, Phys. Rev. B **65**, 085209 (2002).
[19] L. Sangaletti, S. Pagliara, F. Parmigiani, A. Goldoni, L. Floreano, A. Morgante, and V. Aguekian, Phys. Rev. B **67**, 233201 (2003).
[20] O. Rader, C. Pampuch, A. M. Shikin, W. Gudat, J. Okabayashi, T. Mizokawa, A. Fujimori, T. Hayashi, M. Tanaka, A. Tanaka, and A. Kimura, Phys. Rev. B **69**, 075202 (2004).
[21] L. Floreano, G. Naletto, D. Cvetko, R. Gotter, M. Malvezzi, L. Marassi, A. Morgante, A. Santaniello, A. Verdini, F. Tommasini, and G. Tondello, Rev. Sci. Instrum. **70**, 3855 (1999).
[22] L. Floreano, D. Cvetko, G. Bavdek, M. Benes, and A. Morgante, Phys. Rev. B **64**, 075405 (2001).
[23] G. Santoro, S. Scandolo, and E. Tosatti, Phys. Rev. B **59**, 1891 (1999).
[24] H. E. Elsayed-Ali and X. Zeng, Surf. Sci. **538**, 23 (2003).
[25] W. C. Fan and A. Ignatiev, Phys. Rev. B **40**, 5479 (1989).
[26] D. Hobbs, J. Hafner, and D. Spisak, Phys. Rev. B **68**, 014407 (2003).
[27] J. Fink, T. Muller-Heinzerling, B. Scheerer, W. Speier, F. U. Hillebrecht, J. C. Fuggle, J. Zaanen, and G. A. Sawatzky, Phys. Rev. B **32**, 4899 (1985).
[28] B. T. Thole, R. D. Cowan, G. A. Sawatzky, J. Fink, and J. C. Fuggle, Phys. Rev. B **31**, 6856 (1985).
[29] P. S. Bagus, R. Broer, W. A. de Jong, W. C. Nieuwpoort, F. Parmigiani, and L. Sangaletti, Phys. Rev. Lett. **84**, 2259 (2000).
[30] A. E. Bocquet, T. Mizokawa, T. Saitoh, H. Namatame, and A. Fujimori, Phys. Rev. B **46**, 3771 (1992).
[31] S. Plogmann, T. Schlatholter, J. Braun, M. Newmann, Y. M. Yarmoshenko, M. Yablonskikh, E. I. Shreder, E. Z. Kurmaev, A. Wrona, and A. Slebarski, Phys. Rev. B **60**, 6428 (1999).
[32] M. V. Yablonskikh, Yu. M. Yarmoshenko, E. G. Gerasimov, V. S. Gaviko, M. A. Korotin, E. Z. Kurmaev, S. Bartkowski, and M. Neumann, J. Magn. Magn. Mater. **256**, 396 (2003).
[33] L. C. Davis and L. A. Feldkamp, Phys. Rev. B **15**, 2961 (1977).
[34] H. Sato, S. Senba, H. Okuda, M. Nakateke, A. Furuta, Y. Ueda, M. Taniguchi, A. Tanaka, and T. Jo, J. Electron Spectrosc. Relat. Phenom. **88–91**, 425 (1998).
[35] L. Sangaletti, S. Pagliara, F. Parmigiani, A. Goldoni, L. Floreano, A. Morgante, and V. Aguekian, J. Electron Spectrosc. Relat. Phenom. **137–140**, 553 (2004).
[36] S. Hüfner, S.-H. Yang, B. S. Mun, C. S. Fadley, J. Schafer, E. Rotenberg, and S. D. Kevan, Phys. Rev. B **61**, 12582 (2000).
[37] Y. Ishida, D. D. Sarma, K. Okazaki, J. Okabayashi, J. I. Hwang, H. Ott, A. Fujimori, G. A. Medvedkin, T. Ishibashi, and K. Sato, Phys. Rev. Lett. **91**, 107202 (2003).
[38] O. Rader, E. Vescovo, M. Wuttig, D. D. Sarma, S. Blügel, F. J. Himpsel, A. Kimura, K. S. An, T. Mizokawa, A. Fujimori, and C. Carbone, Europhys. Lett. **39**, 429 (1997).
[39] O. Rader, W. Gudat, C. Carbone, E. Vescovo, S. Blügel, R. Klasges, W. Eberhardt, M. Wuttig, J. Redinger, and F. J. Himpsel, Phys. Rev. B **55**, 5404 (1997).
[40] H. A. Dürr, G. van der Laan, D. Spanke, F. U. Hillebrecht, and N. B. Brookes, Phys. Rev. B **56**, 8156 (1997).
[41] M. C. Richter, P. Bencok, R. Brochier, V. Ilakovac, O. Heckmann, G. Paolucci, A. Goldoni, R. Larciprete, J.-J. Gallet, F. Chevrier, G. Van der Laan, and K. Hricovini, Phys. Rev. B **63**, 205416 (2001).
[42] A. Kimura, S. Suga, T. Shishidou, S. Imada, T. Muro, S. Y. Park, T. Miyahara, T. Kaneko, and T. Kanomata, Phys. Rev. B **56**, 6021 (1997).
[43] S. Picozzi, L. Ottaviano, M. Passacantando, G. Profeta, A. Continenza, F. Priolo, M. Kim, and A. J. Freeman, Appl. Phys. Lett. **86**, 6251 (2005).